heavy atoms were located in succeeding difference Fourier syntheses. Hydrogen atoms were located and added to the structures, but their positions were not refined. All calculations, including the full-matrix least-squares refinement, were performed with use of the Enraf-Nonius SDP program package on a VAX computer.

Acknowledgment. We thank the National Science Foundation (Grant CHE-8612063) for support of the research. NSF support for the Crystallographic Unit at Purdue (Grant CHE-8615556) is also gratefully acknowledged.

Supplementary Material Available: Listings of fractional coordinates, anisotropic thermal parameters, and all bond distances and angles (48 pages); listings of observed and calculated structure factors (78 pages). Ordering information is given on any current masthead page.

Synthesis, Structure, Reactivity, and Diastereoisomer Separation of (tropone)$Fe(CO)_2L$ Complexes (L = PPh_3, (+)-Neomenthyldiphenylphosphine)

James A. S. Howell* and Adrian D. Squibb

Department of Chemistry, University of Keele, Keele, Staffordshire ST5 5BG, U.K.

Zeev Goldschmidt, Hugo E. Gottlieb, and Amira Almadhoun

Department of Chemistry, Bar-Ilan University, Ramat-Gan 52100, Israel

Israel Goldberg

Department of Chemistry, Tel-Aviv University, Ramat-Aviv 69978, Israel

Received May 25, 1989

The title complexes have been prepared by amine oxide substitution of (tropone)$Fe(CO)_3$. The solid-state molecular structure of (tropone)$Fe(CO)_2PPh_3$ reveals a distorted-square-pyramidal geometry with a basal PPh_3 trans to the keto-substituted C=C bond; in solution, both basal isomers are populated. Rates of normal and inverse electron demand cycloaddition, and of sigmahaptotropic rearrangement, are much enhanced relative to those for the tricarbonyl. The (tropone)$Fe(CO)_2$((+)-neomenthyldiphenylphosphine) diastereoisomer of 6*S* planar chirality may be isolated by crystallization. Though the rate of the 1,3-shift is enhanced relative to that for the tricarbonyl, normal and inverse electron demand cycloadditions and electrophilic attack proceed under mild conditions without racemization of the planar chirality.

Introduction

Cyclic and acyclic (η^4-polyene)$Fe(CO)_3$ complexes continue to attract attention as intermediates, particularly for asymmetric synthesis.[1] For η^4-triene complexes such as (tropone)- or (cycloheptatriene)$Fe(CO)_3$, interest has centered particularly on the regio- anad stereoselectivity of reactions at the uncoordinated double bond. Thus, (tropone)$Fe(CO)_3$ (**1a**) may be protonated[2] or acylated[3] at C-1 and undergoes 1,2-cycloadduct formation with a variety of reagents, including 3,6-bis(methoxycarbonyl)-1,2,4,5-tetrazine,[4] cyclopentadiene,[5] nitrile oxides[6] or imines,[7] and diazoalkanes.[8] The last has received application in the synthesis of cyclocolorenone[9] and β-thujaplicin,[3] while 1,2-addition of $CpFe(CO)_2(\eta^1$-allyl) complexes to oxygen-alkylated (tropone)$Fe(CO)_3$ provides access to 4-keto-hydroazulenes.[10] Concerted cycloaddition of tetracyanoethylene (TCNE)[11] or 4-phenyltriazoline-3,5-dione (NPTD)[12] results in kinetically controlled, predominant 1,3-addition; isomerization yields the thermodynamically favored 1,5-cycloadducts, which on oxidative decomplexation yield the product of formal 1,4-addition to the free ligand.[13]

Improved preparations of the related $Fe(CO)_2(PR_3)$ derivatives also make these complexes attractive candidates due to their enhanced reactivity toward electrophiles,[14] the greater regiospecificity of the reactions of the derived dienyl salts with nucleophiles,[15] and the possibility

* To whom correspondence should be addressed.

(1) For recent leading references, see: (a) Howard, P. W.; Stephenson, G. R.; Taylor, S. C. *J. Chem. Soc., Chem. Commun.* **1988**, 1603. (b) Pearson, A. J.; Blystone, S. L.; Nar, H.; Pinkerton, A. A.; Roden, B. A.; Yoon, J. *J. Am. Chem. Soc.* **1989**, *111*, 134. (c) Nunn, K.; Mosset, P.; Gree, R.; Saalfrank, R. W. *Angew. Chem., Int. Ed. Engl.* **1988**, *27*, 1188.

(2) (a) Eisenstadt, A. *J. Organomet. Chem.* **1975**, *97*, 443. (b) Brookhart, M. S.; Lewis, C. P.; Eisenstadt, A. *J. Organomet. Chem.* **1977**, *127*, C14 and references therein.

(3) Franck-Neumann, M.; Brion, F.; Martina, D. *Tetrahedron Lett.* **1978**, 5033.

(4) Ban, T.; Nagai, K.; Miyamoto, Y.; Haramo, K.; Yasuda, M.; Kanematsu, K. *J. Org. Chem.* **1982**, *47*, 110.

(5) Franck-Neumann, M.; Martina, D. *Tetrahedron Lett.* **1977**, 2293.

(6) Bonadeo, M.; Gandolfi, R.; de Micheli, C. *Gazz. Chim. Ital.* **1977**, *107*, 577.

(7) Bonadeo, M.; de Micheli, C.; Gandolfi, R. *J. Chem. Soc., Perkin Trans. 1* **1977**, 930.

(8) Johnson, B. F. G.; Lewis, J.; Wege, D. *J. Chem. Soc., Dalton Trans.* **1976**, 1874.

(9) Saha, M.; Bagby, B.; Nicholas, K. M. *Tetrahedron Lett.* **1986**, *27*, 915.

(10) Watkins, J. C.; Rosenblum, M. *Tetrahedron Lett.* **1984**, *25*, 2097.

(11) (a) Goldschmidt, Z.; Gottlieb, H. E.; Cohen, D. *J. Organomet. Chem.* **1985**, *294*, 219. (b) Chopra, S. K.; Moran, G.; McArdle, P. *J. Organomet. Chem.* **1981**, *214*, C36. (c) Hallinan, N.; McArdle, P.; Burgess, J.; Guardado, P. *J. Organomet. Chem.* **1987**, *333*, 77. (d) Chopra, S. K.; Hynes, M. J.; McArdle, P. *J. Chem. Soc., Dalton Trans.* **1981**, 586.

(12) Goldschmidt, Z.; Gottlieb, H. E.; Almadhoun, A. *J. Organomet. Chem.* **1987**, *326*, 405.

(13) Goldschmidt, Z.; Bakal, Y. *Tetrahedron Lett.* **1977**, 955.

0276-7333/90/2309-0080$02.50/0

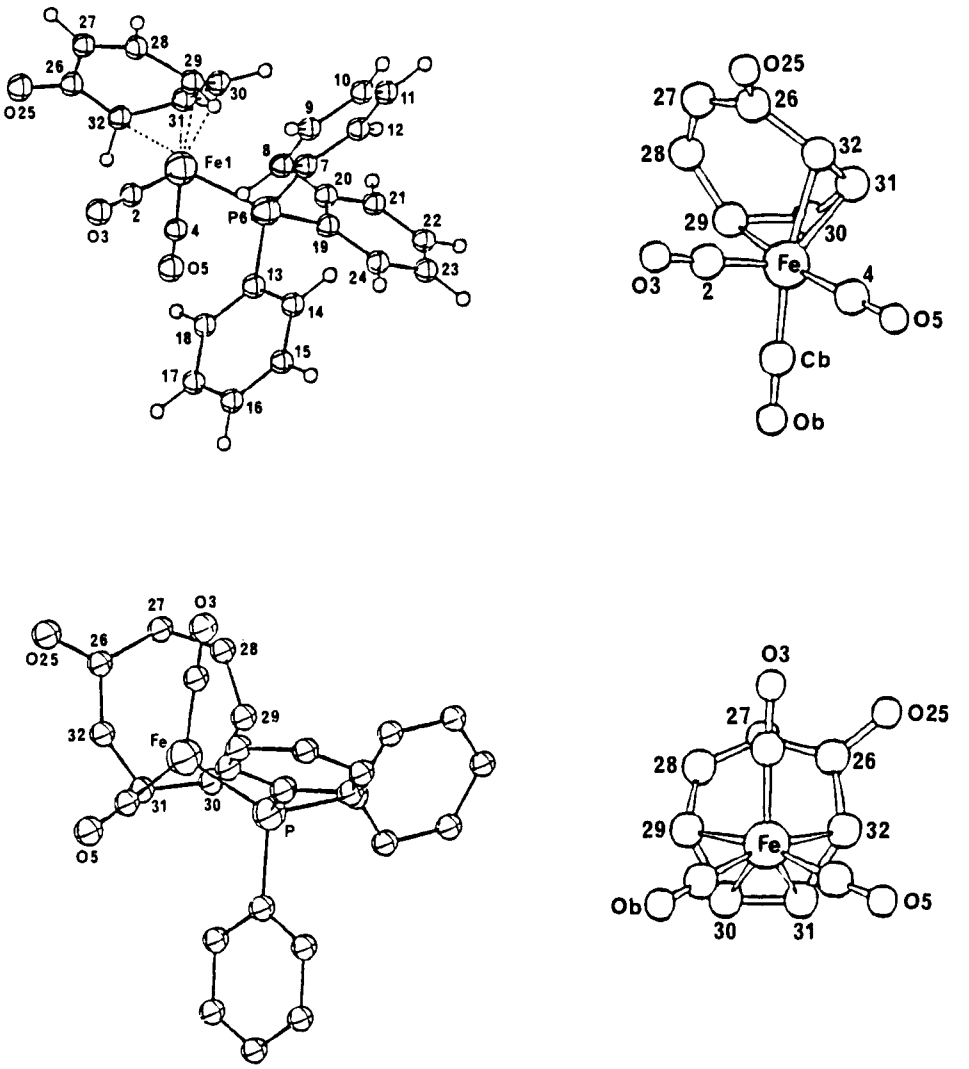

Figure 1. Molecular structures of (right) **1a** and (left) **1b**.

of using a chiral phosphine as a center of induction[16] or resolution.[17] Here, we describe the changes in reactivity induced by phosphine substitution of **1a**, together with full details of the application of (+)-neomenthyldiphenylphosphine (NMDPP) as a resolving center for this chiral complex.

Results

The complexes $(C_7H_6O)Fe(CO)_2PPh_3$ (**1b**), $(C_7H_6O)Fe(CO)_2P(m\text{-}C_6H_4Me)_3$ (**1c**), $(C_7H_6O)Fe(CO)_2P(o\text{-}C_6H_4Me)_3$ (**1d**), and $(C_7H_6O)Fe(CO)_2$((+)-NMDPP) (**1e**) were prepared by trimethylamine oxide substitution of $(C_7H_6O)Fe(CO)_3$ (**1a**).[18]

(a) Solid-State and Solution Structure of 1b. The solid-state molecular structure of **1b** (Figure 1) exhibits the distorted-square-pyramidal structural typical of (diene)$Fe(CO)_3$ complexes; the phosphine ligand occupies the basal position trans to the coordinated keto-substituted C=C bond. Table I lists the most important bond lengths and angles, together with the analogous values for **1a**.[19a] At the 3σ level, there are no significant differences in bond lengths. The major structural changes, which are most probably steric in origin, involve a tilting of the diene relative to the $Fe\text{-}CO_{axial}$ bond such that the axial CO eclipses $C_{27\text{-}28}$ rather than C_{27}, coupled with a marked asymmetry in the $CO_{axial}\text{-}Fe\text{-}L_{basal}$ angles (102.0, 97.3°), which are equivalent (100°) in the tricarbonyl.

Weak nonbonded tropone–PPh_3 interactions are evident in the $C_{7,9}\text{-}C_{29}$ and $C_{7,8}\text{-}C_{30}$ distances of ca. 3.5 Å, an interaction that would be greatly increased in the P(*o*-tolyl)$_3$ complex **1d** (vide infra). Examination of dihedral angles shows little difference in the conformation of the noncoordinated three-carbon fragment; a much more substantial alteration in conformation and decrease in the $C_{26}\text{-}C_{32}\text{-}C_{31}$ angle is observed in (1,2,4,6-tetraphenyltropone)$Fe(CO)_3$[19b] (numbering as in Scheme I) as a result of minimization of nonbonded interaction between the ketonic CO and neighboring phenyl groups.

Fluxionality in solution is evident in the variable-temperature ^{31}P spectra (Figure 2), which show the presence of two populated geometric isomers (1:1.2 ratio in acetone at 225 K, 1:1.6 ratio in dichloromethane at 218 K). The

(14) (a) Birch, A. J.; Raverty, W. D.; Hsu, S. Y.; Pearson, A. J. *J. Organomet. Chem.* **1984**, *260*, C59. (b) Howell, J. A. S.; Tirvengadum, M. C.; Walton, G. *J. Organomet. Chem.* **1988**, *338*, 217.
(15) Pearson, A. J.; Kole, S. L.; Ray, T. *J. Am. Chem. Soc.* **1984**, *106*, 6060.
(16) Howell, J. A. S.; Thomas, M. J. *J. Chem. Soc., Dalton Trans.* **1983**, 1401.
(17) (a) Howell, J. A. S.; Squibb, A. D.; Walton, G.; McArdle, P.; Cunningham, D. *J. Organomet. Chem.* **1985**, *319*, C45. (b) Howell, J. A. S.; Tirvengadum, M. C.; Squibb, A. D.; Walton, G.; McArdle, P.; Cunningham, D. *J. Organomet. Chem.* **1988**, *347*, C5.
(18) Birch, A. J.; Kelly, L. F. *J. Organomet. Chem.* **1985**, *268*, C5.
(19) (a) Dodge, R. P. *J. Am. Chem. Soc.* **1964**, *86*, 5429. (b) Klimes, J.; Weiss, E. *Chem. Ber.* **1982**, *115*, 2175.

Scheme I

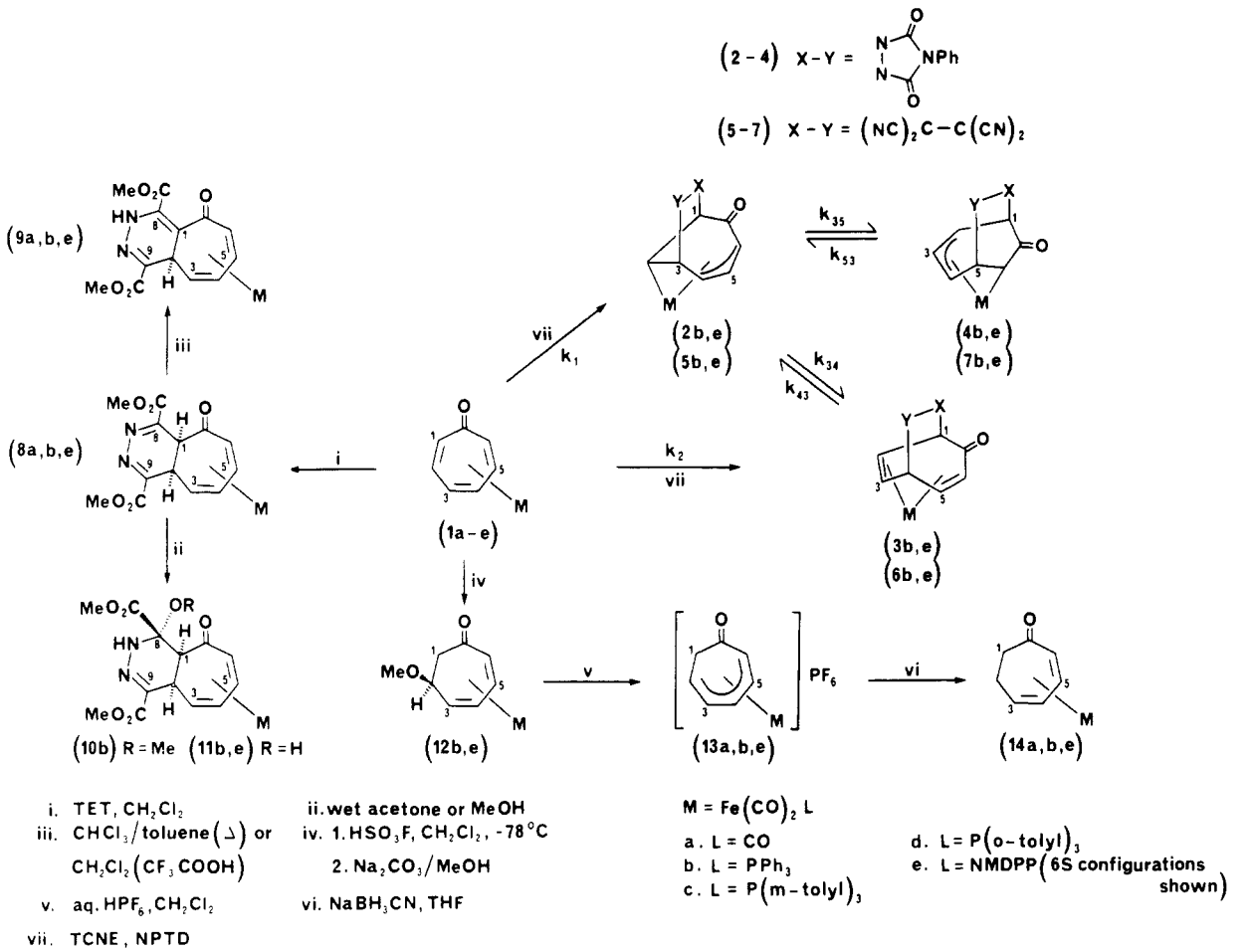

presence of two phosphorus-coupled resonances assignable to axial carbonyls at 221.0 and 221.3 ppm in the low-temperature ^{13}C spectrum (Table II) is consistent with population of the two nonequivalent basal isomers (B/B′) of the distorted-square-pyramidal geometry.[20]

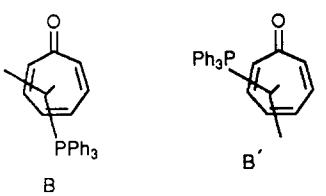

B/B′ exchange does not result in complete carbonyl scrambling, and as expected, *two* CO resonances of the correct averaged chemical shift are observed at 293 K, though their broadness precludes measurement of averaged J(P–C) values. The absence of the phosphine-substituted axial isomer may be attributed to severe steric interaction of phosphine with the uncoordinated three-carbon fragment (C_7–C_1–C_2).

Separate resonances for the two isomers are also seen at low temperature in the organic ^{13}C region and in the ^1H spectrum (Table III, Figure 3). A detailed analysis of the ^1H spectrum reveals that the solid-state conformation B is the *minor* conformer in solution; in particular, the relative upfield shift of $H_{3,4}$ in the minor isomer and $H_{5,6}$ in the major isomer is consistent with shielding by the phenyl rings in B and B′, respectively, while the large J(P–$H_{3,4}$) values observed for the minor isomer are consistent with

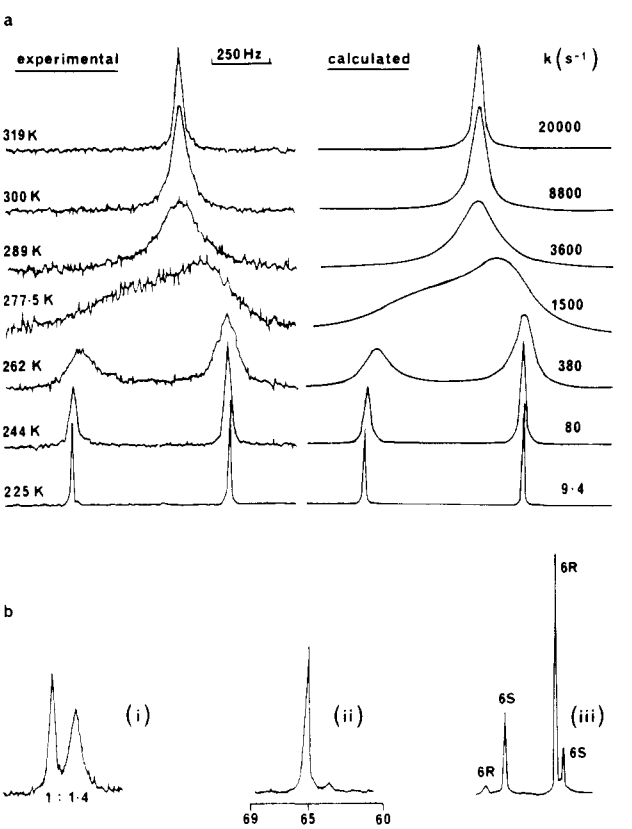

Figure 2. ^{31}P NMR spectra of (a) **1b** in acetone-d_6 and (b) **1e** in CD_2Cl_2 (i, 6*S*, 6*R* equilibrium mixture (273 K); ii, isolated 6*S* diastereoisomer (273 K); iii, 6*S*, 6*R* equilibrium mixture (211 K)).

(20) Howell, J. A. S.; Walton, G. *J. Chem. Soc., Chem. Commun.* **1986**, 622.

Table I. Important Bond Lengths and Angles in 1a and 1b

(a) Bond Lengths (Å)

	1a	1b
Fe–C_2	1.757 (9)	1.762 (6)
Fe–C_4	1.749 (10)	1.776 (7)
Fe–P		2.233 (2)
Fe–C_b[a]	1.771 (10)	
C_2–O_3	1.160 (10)	1.133 (7)
C_4–O_5	1.170 (10)	1.138 (9)
C_b–O_b	1.133 (10)	
Fe–C_{32}	2.113 (9)	2.129 (8)
Fe–C_{31}	2.066 (10)	2.039 (6)
Fe–C_{30}	2.041 (10)	2.037 (2)
Fe–C_{29}	2.148 (10)	2.135 (8)
C_{26}–O_{25}	1.246 (12)	1.220 (10)
C_{26}–C_{32}	1.493 (13)	1.456 (12)
C_{31}–C_{32}	1.442 (13)	1.443 (9)
C_{30}–C_{31}	1.396 (13)	1.391 (10)
C_{29}–C_{30}	1.436 (14)	1.405 (9)
C_{28}–C_{29}	1.463 (14)	1.469 (14)
C_{27}–C_{28}	1.342 (14)	1.336 (12)
C_{26}–C_{27}	1.447 (14)	1.452 (11)

(b) Bond Angles[b] (deg)

	1a	1b
C_2–Fe–C_4	100.4	102.3 (3)
C_2–Fe–P		97.3 (3)
C_2–Fe–C_b	99.5	
C_2–Fe–C_{32}	95.4	100.6 (3)
C_2–Fe–C_{29}	94.2	90.4 (3)
C_2–Fe–C_{31}	133.1	136.9 (3)
C_2–Fe–C_{30}	132.3	129.2 (3)
C_4–Fe–P		88.5 (2)
C_4–Fe–C_b	88.8	
C_4–Fe–C_{32}	90.4	88.5 (3)
C_4–Fe–C_{31}	95.5	95.4 (3)
P–Fe–C_{29}		96.5 (2)
C_b–Fe–C_{29}	92.1	
P–Fe–C_{30}		95.8
C_b–Fe–C_{30}	95.6	
C_{26}–C_{32}–C_{31}	127.5	128.6 (7)
C_{30}–C_{31}–C_{32}	120.4	120.2 (7)
C_{29}–C_{30}–C_{31}	121.4	119.8 (7)
C_{28}–C_{29}–C_{30}	122.2	125.1 (8)
C_{27}–C_{28}–C_{29}	126.9	127.1 (8)
C_{26}–C_{27}–C_{28}	123.8	124.1 (8)
C_{27}–C_{26}–C_{32}	122.9	121.5 (7)
O_{27}–C_{26}–C_{32}	115.5	118.7 (7)
O_{25}–C_{26}–C_{27}	121.3	119.7 (7)
Fe–C_4–O_5	177.1	177.5 (6)
Fe–C_2–O_3	178.3	177.5 (6)
Fe–C_b–O_b	178.1	179.5 (7)

(c) Dihedral Angles

	1a	1b	other[c]
C_{30}–C_{31}–C_{32}–C_{26}	-49.2	-52.7	-58.5
C_{29}–C_{30}–C_{31}–C_{32}	4.5	1.8	-2.8
C_{28}–C_{29}–C_{30}–C_{31}	53.0	52.4	53.2
C_{27}–C_{28}–C_{29}–C_{30}	-48.2	-43.2	-31.9
C_{26}–C_{27}–C_{28}–C_{29}	-7.3	-8.9	-5.2
C_{32}–C_{27}–C_{28}–C_{29}	22.0	14.2	-16.1
C_{31}–C_{32}–C_{26}–C_{27}	23.2	33.8	66.2

[a] C_b–O_b = second basal CO in the tricarbonyl. [b] Standard deviation in angles 0.8–0.9° for **1a**. [c] Value for (1,2,4,6-tetraphenyltropone)Fe(CO)$_3$.

the small P–Fe–C–$H_{3,4}$ dihedral angles in B.

Line-shape analysis of the variable-temperature ^{31}P spectra yields a value of $\Delta G^{\ddagger}(298\ \text{K}) = 51 \pm 4$ kJ mol^{-1}, indistinguishable from the value reported previously for the tricarbonyl.[21] Both the isomer distribution and free energy of activation are, however, sensitive to phosphine cone angle. Thus, although the analogous P(*m*-tolyl)$_3$ complex **1c** exhibits behavior very similar to that of **7b** (isomer ratio 1:1.8 at 208 K), the P(*o*-tolyl)$_3$ complex **1d** (cone angle 194°) exhibits a limiting low-temperature ^{31}P spectrum at only 253 K with an isomer ratio of 1:4.5. *Three* methyl resonances assignable to the P(*o*-tolyl)$_3$ ligand may be observed in the ^{1}H spectrum at 253 K, consistent with a restricted rotation about the Fe–P axis. These resonances broaden and coalesce at a rate similar to that for the coalescence of the B/B′ resonances in the ^{31}P NMR spectrum, though in neither case can a limiting high-temperature spectrum be obtained before decomposition (ca. 333 K). It is possible that B/B′ exchange and Fe–P bond rotation may be synchronous.

These results indicate that the basal position trans to the keto group is sterically the most hindered. All of the η^4-1,3-diene complexes derived from **1b** (Scheme I) also show two resonances in the limiting low-temperature ^{31}P spectra (Table II). With one exception (the tetrazine adduct **8b**), B′ remains the most populated basal isomer. The

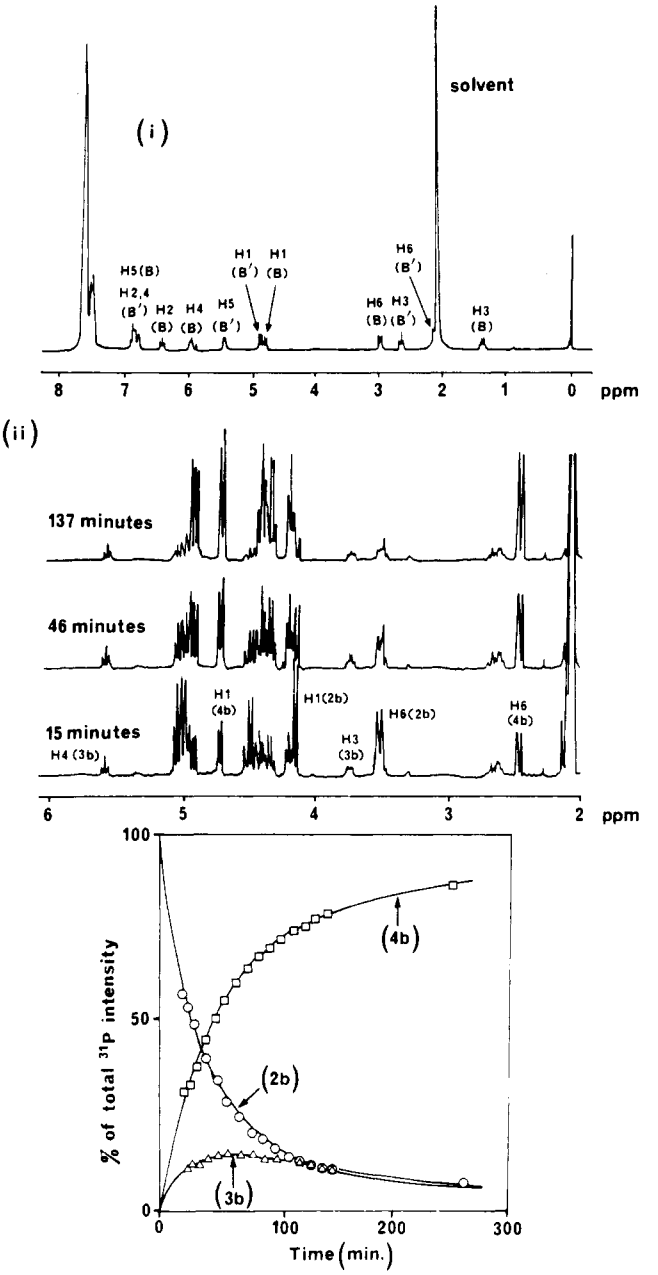

Figure 3. Low-temperature ^{1}H NMR spectra of **1b** and its reaction with NPTD; (i) **1b** in acetone-d_6 at 213 K; (ii) **1b** + NPTD in acetone-d_6 at 264 K.

(21) Kruczynski, L.; Takats, J. *Inorg. Chem.* **1976**, *15*, 3140.

Table II. Spectroscopic Data

		NMR				
		$^1H^b$		$^{13}C^c$		$^{31}P^d$
complex	IR[a]	assignt	δ	assignt	δ	δ
1a		6	3.0 (m)	4, 5	91.0, 95.7	
		4, 5	5.08 (m)	3, 6	51.8, 59.9	
		3	1.70 (t)	1, 2	120.9, 148.2	
		2	5.72 (m)	7	197.5	
		1	4.94 (dq)	CO	207.5 (br)	
				CO	203.1, 204.3, 213.4 [223 K]	
1b	1995	6	2.99 (t)	4, 5	92.8, 96.3	66.0 (br)
	1939	4	5.50 (t)	3, 6	49.0, 61.0 (br)	64.9, 70.1 [218 K] (1.6:1)
		5	4.93 (m)	1, 2	121.3, 149.9	
		3	1.83 (t)	7	200.1	
		2	6.07 (m)	CO	216.9, 215.1 (br)	
		1	5.18 (dq)	CO	221.3 (7.3), 221.0 (7.4), 209.7 (25.6) [215 K]	
1c	1992	6	2.55 (t, br)	4, 5	93.2, 96.4	63.1 (br)
	1934	4	5.83 (m, br)	3, 6	48.6, 61.2 (br)	62.5, 69.7 [208 K] (1.8:1)
		5	5.30 (m, br)	1, 2	123.0, 150.0	
		3	1.93 (q, br)	7	200.3	
		2	6.36 (m)	CO	217.2, 214.9 (br)	
		1	4.76 (dq)	Me	21.4 (br)	
		Me	2.21 (s)			
1d	1988	6	2.91 (t, br)	4, 5	96.2, 99.4 (br)	52.8 (br)
	1932	4	5.65 (t, br)	3, 6	42.5, 63.1 (br)	51.9, 56.0 [253 K] (4.5:1)
		5	4.22 (m, br)	1, 2	122.5, 150.1 (br)	
		3	1.77 (t)	7	201.4	
		2	6.10 (t, br)	Me	23.2 (br)	
		1	5.31 (dq)	Me	21.9 (6.1), 22.9 (3.7) [243 K]	
		Me	1.27 (s)			
			2.40 (s)			
			2.46 (s)			
1e[g]	1984			4, 5	92.6, 89.9 (br) [283 K]	63.2 (br) (6*S*)
	1928			3, 6	49.8, 59.0 (br)	62.7, 64.5 [211 K] (1:1.7)
				1, 2	121.1, 150.7	
				7	206.8	61.7 (br) (6*R*)
14b[h]	1986	1_{exo}	1.70 (m)	4, 5	90.1, 92.5	64.2
	1930	1_{endo}	2.75 (t)	3, 6	57.0 (3.0), 56.8	61.0, 73.3 [198 K] (3.0:1)
		2_{exo}	2.05 (d)	1, 2	36.4, 38.9	
		2_{endo}	2.15 (dd)	7	209.0	
		3	2.58 (t)	CO	215.7 (18.6)	
		6	2.89 (dd)		217.0 (13.7)	
		4	4.80 (t)			
		5	4.25 (m)			
14e[g,i]	1976			4, 5	92.2, 92.9	66.1 (6*S*)
	1922			3, 6	55.3, 58.2	61.2, 69.4 [198 K] (1:2.2)
				1, 2	36.4, 38.9	63.9 (6*R*)
				7	208.8	
13b	2054			2, 6	71.5, 80.3	56.8
	2018			3–5	99.9, 100.7, 103.7	56.9, 58.9 [223 K] (1:1)
				1	33.5	−144 (J(P–F) = 710, PF_6)
				7	191.7	
13e[g]	2048			2, 6	73.9, 80.6	61.5 (6*S*)
	2010			3–5	99.4, 102.6, 105.6	60.7 (6*R*)
				1	33.8	
				7	191.0	
12b	1986			4, 5	89.6, 92.6	65.1
	1928			3, 6	57.3, 57.5	61.8, 70.4 [206 K] (2.9:1)
				1	44.1	
				2	83.8	
				OMe	55.4	
12e[g]	1984			4, 5	91.6, 93.6	67.2 (6*S*)
	1930			3, 6	55.3, 59.3	62.2, 68.9 [198 K] (1:8.3)
				1	44.1	65.1 (6*R*)
				2	84.1 (3.0)	
				OMe	55.4	
8b	1998	4, 5	4.69 (m, br)	4, 5	89.7, 91.5	64.0 (br)
	1946	6	2.71 (m, br)	3, 6	47.5, 54.7 (br)	58.7, 67.9 [213 K] (1:1.6)
		3	1.84 (m, br)	1	41.3	
		1	2.75 (d, 8.0)	2	45.4	
		2	4.03 (dq)	7	203.3	
		CO_2Me	3.69 (s)	CO_2Me	53.2, 53.4	
			3.76 (s)	CO_2Me	152.9, 154.8	
				8, 9	*e*	

Table II (Continued)

		NMR				
		^{1}H[b]		^{13}C[c]		^{31}P[d]
complex	IR[a]	assignt	δ	assignt	δ	δ
8e[g]	1996			4, 5	87.8, 96.2	65.6 (6*S*)
	1942			3, 6	48.8, 52.2	61.6, 68.8 [203 K] (1:8.8)
				1	40.8 (2)	
				2	44.9	63.3 (6*R*)
				7	202.8	
				CO_2*Me*	52.6, 53.0	
				CO_2Me	152.6,154.7	
				8, 9	*e*	
9b	1986	4, 5	5.03 (m)	4, 5	90.3, 92.3	63.7
	1938	6	2.98 (t)	3, 6	55.4, 59.7	60.0, 68.4 [208 K] (1.7:1)
		3	2.65 (m)	2	45.9	
		2	4.90 (s)	7	202.6	
		CO_2Me	3.69 (s)	CO_2*Me*	52.4, 52.8	
			3.80 (s)	*C*O_2Me	160.3, 164.3	
		NH	7.69 (br)	1, 8	121.2, 123.0	
				9	*e*	
9e[g]	1984			4, 5	89.9, 95.8	64.9 (6*S*)
	1930			3, 6	62.9, 53.1 (br)	58.2, 67.0 [203 K] (1:6.9)
				2	46.2 (br)	
				7	203.7	
				CO_2*Me*	52.8	63.3 (6*R*)
				CO_2Me	160.4, 164.1	
				1, 8	121.5, 122.7	
				9	*e*	
10b	1992	4	4.93 (t, br)	4, 5	89.4, 92.7	62.7
	1940	5	4.53 (m, br)	3, 6	46.8, 55.6	59.4, 67.9 [213 K] (4.4:1)
		6	2.84 (t, br)	1, 2	45.9, 46.8	
		3	1.90 (d, br)	7	203.8	
		1, 2	3.38 (d)	8	85.1	
			3.50 (d) AB (8 Hz)	CO_2*Me*	50.6, 53.2	
		CO_2Me	3.70 (s)	*C*O_2Me	163.5, 168.0	
			3.79 (s)	OMe	50.6	
		OMe	3.03 (s)	9	*e*	
		NH	*e*			
11b	1992	4	4.98 (t, br)	4, 5	89.7, 92.2	63.6
	1938	5	4.57 (m, br)	3, 6	47.7, 55.4	59.8, 67.7 [213 K] (2.9:1)
		6	2.83 (t)	1, 2	45.4, 48.3	
		3	1.98 (d, br)	7	205.7	
		1, 2	3.42 (d)	8	81.0	
			3.49 (d) AB (7 Hz)	CO_2*Me*	52.1, 53.3	
		CO_2Me	3.66 (s)	*C*O_2Me	163.7, 169.3	
			3.77 (s)	9	*e*	
		NH	*e*			
11e[g]	1986			4, 5	89.6, 95.4 (br)	66.7 (6*S*)
	1930			3, 6	51.0, 51.6 (br)	64.7, 70.6 [223 K] (1:1.3)
				1, 2	44.9, 49.2	
				7	206.4	62.8 (6*R*)
				8	81.2	
				CO_2*Me*	51.8, 53.1	
				CO_2Me	163.7, 169.5	
				9	*e*	
15	1986	1_{exo}	1.95 (dd)	3, 4	86.3, 86.6	69.9
	1930	1_{endo}	2.55 (dd)	2, 5	53.0, 63.0	61.7, 70.1 [193 K] (1:3.0)
		2	2.35 (m)	1	39.6	
		5	3.05 (t)	6	193.3	
		3	4.79 (m)	CO	214.9 (20.8)	
		4	4.68 (m)		216.4 (14.7)	
		CH_3CO_2Et	3.92 (q)			
			3.92 (s)			
			1.62 (s)			
7b	2022	1	3.34 (dd)[f]			62.0
	1974	6	2.25 (dq)			
		4, 5	3.63 (m)			
		2	3.91 (t)			
		3	4.34 (q)			
7e[g]	2014	1	3.20 (dd)[f]			64.4 (6*S*, 6*R*)
	1966	6	*f*			
		4, 5	3.31 (m)			
		2	3.55 (t)			
		3	4.01 (q)			

Table II (Continued)

complex	IR[a]	NMR ^1H[b] assignt	^1H[b] δ	^{13}C[c] assignt	^{13}C[c] δ	^{31}P[d] δ
4b	2012	6	2.48 (t)			62.4
	1960	4	3.86 (m)			
		2, 3	4.20 (m)			
		1, 5	4.48 (m)			
4e[g]	2006	6	2.40 (dd)			68.7 (6*S*)
	1956	3, 4	3.89 (m, br)			68.5 (6*R*)
		1, 2, 5	4.61–4.86 (m)			

[a] In cm^{-1}; CH_2Cl_2 solution. [b] In ppm from TMS; benzene-d_6 solution unless stated otherwise. [c] In ppm from TMS; $CDCl_3$ solution at 298 K unless stated otherwise; J(P–C) values (Hz) in parentheses. [d] In ppm from 85% H_3PO_4; CD_2Cl_2 solution at 298 K unless stated otherwise. [e] Under Ph resonance. [f] Acetone-d_6 solution. [g] Only $^1H/^{13}C$ resonances of 6*S* diastereoisomer listed. [h] PPh_3 resonances (ppm): ^{13}C, 128–135 (m); ^1H, 6.9–7.6 (m). Other PPh_3 complexes are similar. [i] NMDPP resonance ppm (J, Hz)): ^{13}C, 17.6, 20.0, 21.0 (11.7), 23.7, 28.1 (6.8), 28.7, 30.4 (4.0), 30.9 (6.9), 36.9 (22.5), 39.5 (br), 127.3–135.5 (m); ^1H, 0.25 (Me, 6.8), 0.93, 1.20 ($CHMe_2$, 6.8), 1.5–3.0 (m), 6.9–7.8 (m). Other NMDPP complexes are similar.

Table III. Low-Temperature Spectroscopic Data for 1b and in Situ Reactions of 1b,e with TCNE and NPTD[a]

complex	H1	H2	H3	H4	H5	H6	^{31}P
1a (acetone, 293 K)	4.94	6.69	2.96		6.67	3.16	
1b (B) (acetone, 213 K)	4.79	6.43	1.34	5.98	6.87	3.00	69.5
	J(5,6) = 8.0, J(4,6) = 1, J(1,6) = 2, J(4,5) = 5, J(3,5) = 0.5, J(3,4) = 7, J=4,P) = 7, J(2,3) = 8, J(1,3) = 0.5, J(3,P) = 8, J(1,2) = 11						
1b (B′)	4.88	6.88	2.60	6.80	5.46	2.16	64.2
	J(5,6) = 7.5, J(4,6) = 1, J(1,6) = 1.5, J(4,5) = 4.5, J(3,5) = 1, J(5,P) = 5.5, J(3,4) = 7, J(2,3) = 8, J(1,3) = 0.5, J(1,2) = 11						
2b (acetone, 264 K)	4.15	2.10	5.05	5.00	4.50	3.52	55.2
	J(1,6) = 2, J(1,2) = 8.5, J(5,6) = 9.5, J(4,6) = 2.5, J(4,5) = 6.5, J(3,5) = 1, J(5,P) = 9, J(3,4) = 6, J(2,4) = 1.5, J(2,3) = 9, J(2,P) = 1.5						
3b (acetone, 264 K)	4.97	3.49	3.73	5.59	2.67	2.61	78.5
	J(1,2) = 8, J(5,6) = 8, J(6,P) = 4, J(4,5) = 7.5, J(5,P) = 3, J(3,4) = 7.5, J(2,3) = 6, J(3,P) = 3.5						
4b (acetone, 264 K)	4.72	4.42	4.35	4.20	4.93	2.46	61.3
	J(1,6) = 2.5, J(1,2) = 7.5, J(5,6) = 9.5, J(4,6) = 1, J(4,5) = 6.5, J(3,5) = 1, J(3,4) = 6, J(2,4) = 3, J(2,3) = 7.5, J(3,P) = 7, J(2,P) = 3						
5b (CH_2Cl_2, 213 K)							54.9
6b (CH_2Cl_2, 213 K)							76.9
7b (CH_2Cl_2, 213 K)							62.2
(6*S*)-**2e** (acetone, 273 K)							61.5
(6*S*)-**2e** (acetone, 193 K)							61.2, 62.9 (1:1)
(6*R*)-**4e** (acetone, 273 K)							61.6
(6*R*)-**4e** (acetone, 193 K)							62.0
(6*S*)-**4e** (acetone, 283 K)							69.4
(6*S*)-**4e** (acetone, 193 K)							69.7, 70.3 (4.4:1)
(6*R*)-**4e** (acetone, 273 K)							68.9
(6*R*)-**4e** (acetone, 193 K)							69.2, 70.2 (3:1)
(6*S*)-**5e** (CH_2Cl_2, 273 K)							57.6
(6*S*)-**5e** (CH_2Cl_2, 218 K)							57.8
(6*R*)-**5e** (CH_2Cl_2, 273 K)							57.6
(6*R*)-**5e** (CH_2Cl_2, 218 K)							57.8
(6*S*)-**7e** (CH_2Cl_2, 273 K)							64.4
(6*S*)-**7e** (CH_2Cl_2, 218 K)							64.5, 65.2 (1:1)
(6*R*)-**7e** (CH_2Cl_2, 273 K)							64.4
(6*R*)-**7e** (CH_2Cl_2, 218 K)							64.7

[a] In ppm with J values given in Hz.

relative stability of B/B′ is, however, quite sensitive to ring size; thus, (cyclohexadienone)$Fe(CO)_2PPh_3$ (**15**), containing one less CH_2 group than **14b**, exhibits a considerably enhanced stability of the B isomer.

(b) Cycloaddition Reactions of 1b. The reaction of **1a** with 4-phenyltriazoline-3,5-dione (NPTD) has recently been studied in detail[12] and proceeds (Scheme I) via kinetically controlled 1,3- and 1,4-addition to give **2b** and **3b**, respectively (k_1/k_2 = 3 at 297 K), followed by thermodynamic equilibration of **2b** and **3b** ([2,2]-sigmahaptotropic shift) and of **2b** with the thermodynamically most stable 1,5-adduct **4b** ([3,3]-sigmahaptotropic shift). Cycloaddition of **1b** with NPTD is too fast to measure by NMR spectroscopy at 297 K but may be monitored at 237 K by ^{31}P NMR methods (see Experimental Section); the three cycloadducts yield distinct, single resonances down to 193 K (Table III) that are well separated from the two resonances of **1b** at this temperature.

The data clearly show (a) an increased kinetic periselectivity compared to that of **1a** since only the 1,3-adduct is formed initially with **1b** and (b) an acceleration in the rate of cycloaddition by ca. 5×10^2 (k_1(**1a**) = 1.56×10^{-3} mol^{-1} dm^3 s^{-1} at 297 K; k_1(**1b**) = 1.23×10^{-2} mol^{-1} dm^3 s^{-1} at 237 K). Thermodynamic equilibration via sigmahaptotropic shift occurs only at higher temperature (264 K) and may be monitored by ^{1}H NMR spectroscopy (Table III, Figure 3), which also provides an unambiguous structural identification of the three cycloadducts. Of particular note and utility are the higher field resonances assignable to H_2 and H_6 of **2b** and **4b** and the coordinated diene pair $H_{5,6}$ of **3b**. The four rate constants of Scheme I may be obtained by a computer fitting of the relevant proton integrals to the rate equations

$$\frac{d[\mathbf{3b}]}{dt} = k_{34}[\mathbf{2b}] - k_{43}[\mathbf{3b}]$$

$$\frac{d[\mathbf{4b}]}{dt} = k_{35}[\mathbf{2b}] - k_{53}[\mathbf{4b}]$$

The good correlation is illustrated in Figure 3 and shows that, relative to the tricarbonyl, the rates of both the [2,2]- and [3,3]-sigmahaptotropic shifts are enhanced by approximately 50-fold, though the thermodynamic equilibrium ratio of the cycloadducts is little affected:

	1b (acetone, 264 K)	**1a** (acetone, 297 K)
k_{35}, s^{-1}	2.8×10^{-4}	2.9×10^{-5}
k_{53}, s^{-1}	1.2×10^{-5}	1.5×10^{-6}
k_{34}, s^{-1}	8.3×10^{-5}	9.8×10^{-6}
k_{43}, s^{-1}	1.3×10^{-4}	2.0×10^{-5}

Attempts to measure similar parameters for the cycloaddition and rearrangement in the reaction of **1b** with tetracyanoethylene (TCNE) were frustrated by the extremely fast rate of cycloaddition (complete within mixing time at 223 K) and precipitation of the 1,5-adduct **7b** in the later stages of reaction. Qualitatively, reaction of **1b** with TCNE in CH_2Cl_2 at 223 K yields an 8:1 mixture of **5b** and **6b** that on warming to 253 K isomerizes to an 7:1 equilibrium mixture of **7b** and **5b** with disappearance of the 1,4-adduct **6b**. Comparison with the tricarbonyl[11a] thus also shows an enhanced rate of sigmahaptotropic rearrangement and a greatly enhanced rate of cycloaddition. The ordering of the rates of cycloaddition (NPTD < TCNE, also observed for **1a**) is usually inverted in most Diels–Alder reactions,[22] though hindered dienes such as anthracene are known to react with NPTD more slowly than TCNE.[23]

The rate of inverse electron demand cycloaddition of **1b** with 3,6-bis(methoxycarbonyl)-1,2,4,5-tetrazine (TET) is also increased relative to that for the tricarbonyl. Accurate in situ ^{31}P NMR monitoring is frustrated by N_2 evolution and the broadness of reactant and product resonances above 243 K, but comparison of an approximate second-order rate constant for the reaction of **1b** with TET in CH_2Cl_2 at 253 K (ca. 10^{-2} mol^{-1} dm^3 s^{-1}) with that reported for **1a** in CH_3CN at 307 K (7.1×10^{-3} mol^{-1} dm^3 s^{-1})[4] indicates an acceleration of approximately 10^2. For **1a**, tautomerization occurs under the reaction conditions to yield the 1,4-dihydropyridazine **9a** as the isolated product; this is a general phenomenon, and only in a few cases have the initial 1,5-dihydropyridazine adducts been isolated.[24]

For **1b**, the acceleration of the cycloaddition allows the isolation of the initial adduct **8b** in good yield. It may be structurally distinguished from **9b** by the *two* saturated ^{13}C resonances and by the strongly coupled $H_{1,2}$ pair (J = 8 Hz) with H_2 also showing smaller couplings to $H_{3,4}$. The irreproducibility of the rate of conversion of **8b** to **9b** may be attributed to acid catalysis; tautomerization is complete within minutes upon addition of a trace of CF_3COOH at 293 K. Dipolar 1,2-addition to one C=N bond is evident in the stereo- and regioselective reactions of **8b** with water and methanol to give **10b** and **11b**.[25] Though single diastereoisomers are isolated, NMR spectra do not provide an unambiguous assignment; the stereoselectivity shown is based on the folded cis-ring structure evident in the crystal structure of the cycloheptatriene analogue of **9a**,[4] while the regiochemistry seems most consistent with the observed, known regioselective tautomerization to **9b**.

The increased rates of cycloaddition in both cases are consistent with a frontier molecular orbital approach,[11a,12,26,27] which shows the primary bonding in (tropone)Fe(CO)$_3$ to involve the HOMO(tropone)–LUMO(Fe(CO)$_3$) and LUMO(tropone)–HOMO(Fe(CO)$_3$) interactions **11** and **17** (Chart I). The former is mainly ligand centered and therefore dominant in orbital-controlled cycloaddition reactions at the organic site. Thus, interaction of **16** with the LUMO of uniparticulate electrophiles is consistent with the predominant 3 + 2 kinetic periselectivity,[26] while **16** also possesses the right symmetry for the LUMO(diene)-controlled inverse electron demand 4 + 2 addition of TET. The expected increase in energy of the Fe(CO)$_3$ valence orbitals on replacement of CO by PR_3 will decrease the tropone–metal interaction in **16**, thus decreasing also the energy separation between **16** and the LUMO of TET, TCNE, and NPTD. Qualitatively, evidence shows that Fe(CO)$_3$ in (diene)Fe(CO)$_3$ complexes is a net electron donor,[28] an effect which is enhanced by substitution of CO by stronger σ-donors.

A rationale for the influence of phosphine substitution on the rates of the sigmahaptotropic shift is not as obvious, though an orbital analysis of the [3,3]-sigmahaptotropic shift has been published.[11a] This acceleration of haptotropic exchange is not unique, however, and the rates of 1,3-metal shift in (tropone)Fe(CO)$_3$ (vide infra) and linear trienes such as **18**, and the racemization of complexes such as **19**, are also accelerated by phosphine substitution.[29]

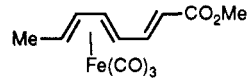

18

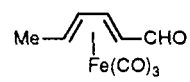

19

(c) Diastereoisomer Separation and Reactivity of (tropone)Fe(CO)$_2$(NMDPP). The planar chirality of (tropone)Fe(CO)$_3$ was demonstrated for the first time by selective enantiomer photolysis with circularly polarized light.[30] Since then, a small-scale separation of enantiomers by HPLC has been achieved,[31] and subsequent to prelim-

(22) Cookson, R. C.; Gilani, S. S. H.; Stevens, I. D. R. *J. Chem. Soc. C* **1967**, 1905.
(23) Sauer, J.; Schroder, B. *Chem. Ber.* **1967**, *100*, 678.
(24) For recent reviews, see: (a) Boger, D. L. *Chem. Rev.* **1986**, *86*, 781. (b) Neunhoffer, H. *Comprehensive Heterocyclic Chemistry*; Pergamon: London, 1984; Vol. 3, pp 550–555.
(25) For similar addition in diazanorcaradienes, see: (a) Steigel, A.; Sauer, J.; Kleier, D. A.; Binsch, G. *J. Am. Chem. Soc.* **1972**, *94*, 2770. (b) Maier, G.; Heep, U. *Chem. Ber.* **1968**, *101*, 1371. (c) Maier, G.; Seidler, F. *Chem. Ber.* **1966**, *99*, 1236.
(26) Chopra, S. K.; Cunningham, D.; Kavanagh, S.; McArdle, P.; Moran, G. *J. Chem. Soc., Dalton Trans.* **1987**, 2927.
(27) Karel, K. J.; Albright, T. A.; Brookhart, M. *Organometallics* **1982**, *1*, 419.
(28) Ittel, S. D.; van Catledge, F. A.; Jesson, J. P. *J. Am. Chem. Soc.* **1979**, *101*, 6905.
(29) Goldschmidt, Z.; Howell, J. A. S. Unpublished results.
(30) Litman, S.; Gedanken, A.; Goldschmidt, Z.; Bakal, Y. *J. Chem. Soc., Chem. Commun.* **1978**, 983.
(31) Tajiri, A.; Morita, N.; Asao, T.; Hatano, M. *Angew. Chem., Int. Ed. Engl.* **1985**, *24*, 329.

Chart I

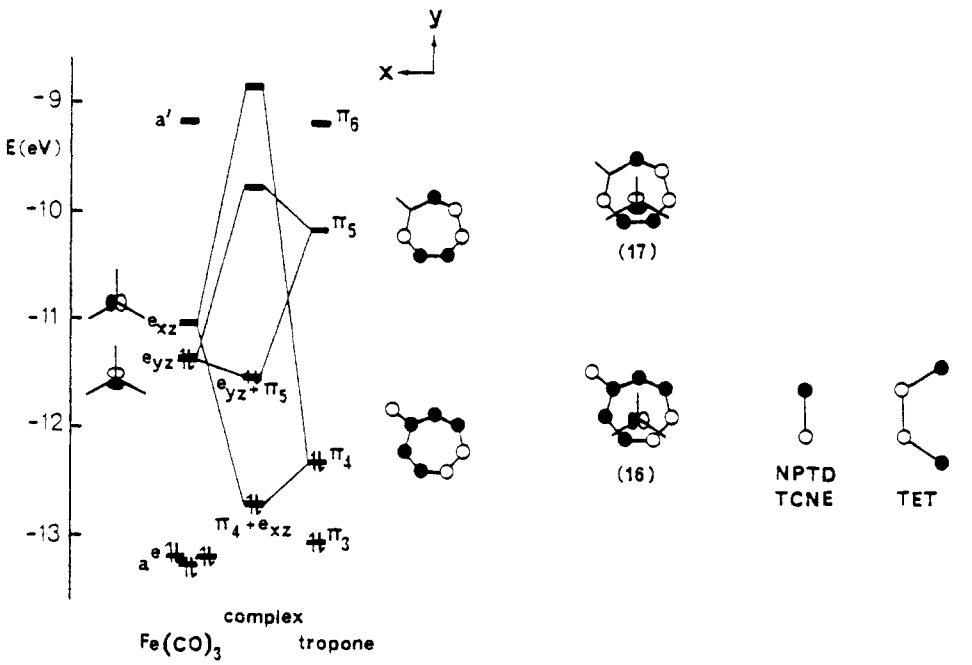

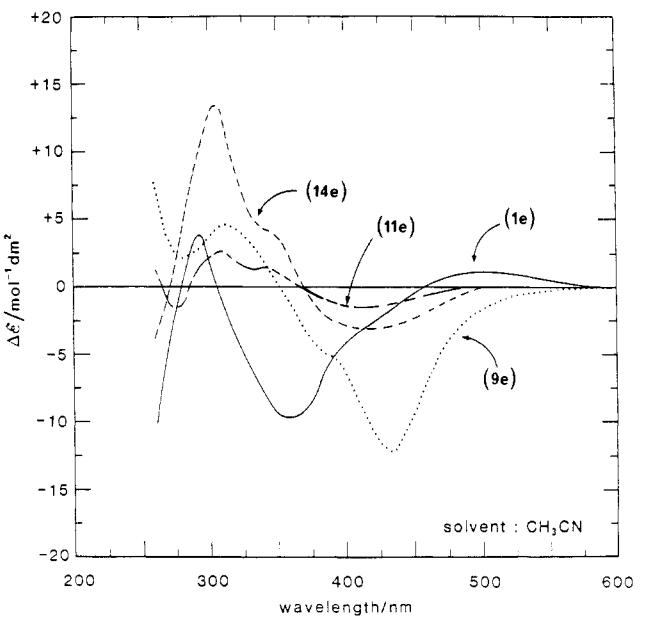

Figure 4. CD spectra of 6*S* isomers of **1**, **9**, **11**, and **14e**.

inary communication of our work,[17a] a resolution based on attack of chiral nucleophiles on **13a** has been reported.[32]

Substitution of **1a** by NMDPP yields **1e**, whose ^{31}P NMR spectrum (Figure 2) reveals an unequal population of two diastereoisomers, from which the less abundant isomer may be isolated by crystallization. A single recrystallization reproducibly yields material of 90–95% diastereoisomeric purity, which is suitable for synthetic purposes since the small amounts of second diastereoisomer carried through may be removed by crystallization of reaction products that are not subject to the racemization by the 1,3-shift which occurs in **1e**. Diastereoisomer equilibration occurs at room temperature over several hours to yield an equilibrium mixture (1.4:1) which is identical with that obtained from the crude reaction product. Differential broadening of the ^{31}P resonances at 273 K is due to slowing of isomer interconversion, and at 211 K, each diastereoisomer exhibits two sharp resonances (Figure 2), which, by analogy with the case for **1b**, may be assigned to unequal populations of the B/B′ pair of each diastereoisomer. A limiting high-temperature spectrum may be obtained in toluene at 333 K, but no reversible line broadening of the diastereoisomeric pair is observed below the temperature of decomposition (ca. 383 K). The difference in thermodynamic stability of the two diastereoisomers is reflected in the greatly differing B:B′ ratios in the two diastereoisomers. The B:B′ ratio of 1.7:1 of the isolated diastereoisomer is more or less maintained in the η^4-diene products derived from it in Scheme I.

In $CDCl_3$, the rate of diastereoisomer interconversion via 1,3-metal shift ($k_1 + k_{-1} = 6.8 \times 10^{-4}$ s^{-1} at 306 K, see Experimental Section) is about 1 order of magnitude faster than that reported for the tricarbonyl ($k = 2.7 \times 10^{-4}$ s^{-1} at 338 K).[31] These results seem consistent with a molecular orbital analysis of the 1,3-shift,[27] which shows that in the lowest energy pathway via the 16e species **20** the major loss

20

of overlap is between the HOMO of tropone and the LUMO of the $Fe(CO)_3$ fragment. As this stabilization in the η^4 ground state (represented by **16**) is expected to be relatively less in **1b** as compared to the case for **1a**, the barrier to 1,3-shift is correspondingly reduced. In a qualitative way, substitution of CO by phosphine stabilizes the electron-deficient η^2 intermediate.

In structurally similar (diene)$Fe(CO)_3$ or [(dienyl)Fe$(CO)_3$]X complexes, the sign of the lowest energy circular dichroism (CD) transition has been proposed as diagnostic of the absolute configuration;[32,33] spectra of diastereoiso-

(32) Morita, N.; Asao, T.; Sotokawa, H.; Hatano, M.; Tajiri, A. *J. Organomet. Chem.* **1988**, *339*, C1.

(33) (a) Alcock, N. W.; Crout, D. H. G.; Henderson, C. M.; Thomas, S. E. *J. Chem. Soc., Chem. Commun.* **1988**, 746. (b) Tajiri, A.; Sotokowa, H.; Morita, N.; Kabuto, C.; Hatano, M.; Asao, T. *Tetrahedron Lett.* **1987**, *28*, 6465. (c) Stephenson, G. R.; Atton, J. G.; Evans, D. J.; Kane-Maguire, L. A. P.; *J. Chem. Soc., Chem. Commun.* **1984**, 1246.

mers of the type (diene)Fe(CO)$_2$(NMDPP) are also essentially mirror image in this region and bear a close similarity to the spectrum of the tricarbonyl of the same planar chirality.[17] The strong negative CD absorption at 360 nm shown by the isolated diastereoisomer of **1e** (Figure 4) clearly shows it to have the same planar chirality as (−)-**1a**.[31] A recent crystallographic determination of the absolute configuration of (+)-**14a**[34] thus allows an assignment of 6*S* absolute stereochemistry to the isolated diastereoisomer of **1e** (based on the numbering of Scheme I; designated 2*S* in the numbering scheme of ref 34). All the reactions of (6*S*)-**1e** outlined in Scheme I yield single diastereoisomeric products whose absolute stereochemistry may be assigned as shown on the basis of the known regio- and stereoselectivity of the reactions. Reaction of an equilibrated (6*S*,*R*)-**1e** mixture shows that, in all but one case, the product derived from the 6*R* diastereoisomer may be easily distinguished by ^{31}P NMR spectroscopy (Table II). For the η^4-diene complexes **1e**, **8e**, **9e**, **11e**, and **14e**, broadness and overlap of all but the inner diene resonances with those of the neomenthyl group limit the utility of ^{1}H NMR spectroscopy in structural assignment; ^{13}C spectra are, however, unambiguous and closely resemble those of the PPh$_3$ complexes. The σ,π-allyl adducts **4b,e** and **7b,e** are too insoluble to permit recording of ^{13}C spectra.

Cycloaddition reactions of (6*S*)-**1e** parallel those of **1b**. Reaction with an equimolar amount of TET is complete within 1 h at 253 K to yield the adduct (6*S*)-**8e**, which undergoes acid-catalyzed tautomerization to give (6*S*)-**9e** or hydration to give (6*S*)-**11e**; CD spectra (Figure 4) show clearly the retention of planar chirality during these transformations. Reaction of (6*S*)-**1e** with TCNE in CH_2Cl_2 is complete within mixing time at 228 K to yield predominantly **2e**, which when it is warmed to 253 K isomerizes without racemization to a 7.2:1 equilibrium mixture of **4e** and **2e**. Similarly, reaction of (6*S*)-**1e** with NPTD in acetone is complete within 1 h at 223 K to yield predominantly **5e**, which on warming to 273 K isomerizes without racemization to an 7.1:1 equilibrium mixture of **7e** and **5e**. In neither case can the 1,4-adducts **3e** and **6e** be detected, either as kinetic products or at thermodynamic equilibrium. At room temperature, all of the σ,π-allyl adducts show single ^{31}P resonances indicative of a single site occupancy within the pseudooctahedral geometry. Though the ^{31}P NMR spectra of the PPh$_3$ complexes show no temperature dependence, the singlet resonances of several of the NMDPP diastereoisomers show a broadening on cooling and resolution into two resonances at low temperature (Table III). Since site interconversion in the pseudooctahedron does not occur on the NMR time scale,[35] the doubled resonances seem most likely associated with inequivalent isomers resulting from restriction of rotation about the Fe–P bond.

Finally, we have examined the possibility of racemization during electrophilic attack (protonation) on **1e**. Protonation of the tricarbonyl at low temperature is known to give initially the hydroxytropylium cation **21a**, which isomerizes to **22a** on warming, with protonation occurring endo at the uncoordinated double bond. Indirect evidence suggests that though racemization via 1,2-shifts is slow in **21a** ($t_{1/2}$ ca. 30 min at 313 K), the rate is considerably enhanced by alkyl substitution of **1a** and considerably reduced by PPh$_3$ substitution of **1a**.[36] Protonation of **1b** or (6*S*)-**1e** with HSO$_3$F at 195 K yields initially the dark red-brown hydroxytropylium cations **21b,e**, which on standing for a few minutes isomerize to the light yellow **22b,e**; neutralization with Na$_2$CO$_3$/MeOH at low tem-

Table IV. Atomic Positional and Thermal Parameters of Compound 1b[a]

atom	*x*/*a*	*y*/*b*	*z*/*c*	U_{eq}, Å^2
Fe_1	0.7752 (1)	0.2575 (1)	0.3211 (1)	0.0322 (3)
C_2	0.7865 (8)	0.1108 (7)	0.4483 (6)	0.0439 (30)
O_3	0.7927 (7)	0.0165 (5)	0.5304 (4)	0.0776 (27)
C_4	0.5772 (8)	0.2642 (6)	0.3079 (5)	0.0424 (27)
O_5	0.4486 (6)	0.2698 (5)	0.3028 (5)	0.0675 (29)
P_6	0.8467 (2)	0.1685 (1)	0.1915 (1)	0.0318 (6)
C_7	1.0565 (6)	0.1417 (4)	0.1469 (4)	0.0408 (30)
C_8	1.1391 (6)	0.2296 (4)	0.0408 (4)	0.0718 (41)
C_9	1.3021 (6)	0.2121 (4)	0.0115 (4)	0.1019 (62)
C_{10}	1.3825 (6)	0.1066 (4)	0.0883 (4)	0.0896 (61)
C_{11}	1.2999 (6)	0.0186 (4)	0.1944 (4)	0.0857 (49)
C_{12}	1.1369 (6)	0.0362 (4)	0.2236 (4)	0.0669 (41)
C_{13}	0.7794 (5)	0.0003 (4)	0.2443 (4)	0.0359 (26)
C_{14}	0.8669 (5)	−0.0909 (4)	0.2030 (4)	0.0701 (41)
C_{15}	0.8171 (5)	−0.2189 (4)	0.2465 (4)	0.0829 (48)
C_{16}	0.6798 (5)	−0.2555 (4)	0.3314 (4)	0.0666 (37)
C_{17}	0.5924 (5)	−0.1643 (4)	0.3728 (4)	0.0550 (32)
C_{18}	0.6422 (5)	−0.0363 (4)	0.3292 (4)	0.0490 (30)
C_{19}	0.7816 (6)	0.2589 (3)	0.0510 (4)	0.0407 (27)
C_{20}	0.7908 (6)	0.2001 (3)	−0.0262 (4)	0.0615 (37)
C_{21}	0.7490 (6)	0.2743 (3)	−0.1352 (4)	0.0739 (40)
C_{22}	0.6981 (6)	0.4073 (3)	−0.1669 (4)	0.0603 (36)
C_{23}	0.6889 (6)	0.4662 (3)	−0.0896 (4)	0.0590 (36)
C_{24}	0.7307 (6)	0.3920 (3)	0.0193 (4)	0.0495 (31)
C_{25}	0.6823 (7)	0.3894 (7)	0.5812 (5)	0.0852 (34)
C_{26}	0.7704 (9)	0.3758 (7)	0.4974 (6)	0.0554 (36)
C_{27}	0.9361 (10)	0.3407 (8)	0.4997 (7)	0.0641 (42)
C_{28}	1.0359 (9)	0.3005 (8)	0.4232 (7)	0.0603 (40)
C_{29}	1.0056 (8)	0.3010 (7)	0.3158 (7)	0.0531 (36)
C_{30}	0.9274 (9)	0.4052 (7)	0.2347 (6)	0.0537 (34)
C_{31}	0.7806 (9)	0.4557 (6)	0.2733 (6)	0.0529 (32)
C_{32}	0.7066 (8)	0.3988 (6)	0.3957 (6)	0.0464 (30)

[a] U_{eq} is one-third of the traceof the orthogonalized U_{ij} tensor. The phenyl substituents were refined and geometrically constrained rigid groups.

Table V

time, s	% of total integrated ^{31}P NMR intens **1b**	**2b**	**3b**	**4b**
0	100	0	0	0
720	87	12	0.9	0
1330	75	25	0.2	0
1940	72	28	0.3	0
2550	64	36	0.2	0
3160	62	37	0.8	0
3770	61	36	1.2	1.9
4330	60	38	1.0	0.9
5600	57	42	0.9	0.8
6210	56	42	1.1	0.9

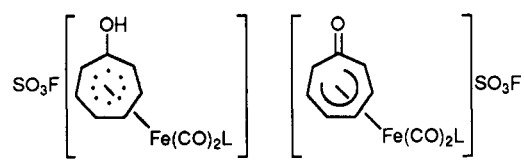

21b, e **22b, e**

(34) Sotokawa, H.; Tajiri, A.; Morita, N.; Kabuto, C.; Hatano, M.; Asao, T. *Tetrahedron Lett.* **1987**, *28*, 5873.

(35) The ^{13}C spectrum of the tricarbonyl analogue of **7b** exhibits three CO resonances at room temperature.[11a]

(36) (a) Eisenstadt, A.; Winstein, S. *Tetrahedron Lett.* **1971**, 613. (b) Brookhart, M. S.; Lewis, C. P.; Eisenstadt, A. *J. Organomet. Chem.* **1977**, *127*, C14. (c) Hunt, D. F.; Farrant, G. C.; Rodeheaver, G. T. *J. Organomet. Chem.* **1972**, *38*, 349. (d) Eisenstadt, A. *J. Organomet. Chem.* **1975**, *97*, 443. (e) Lewis, C. P.; Kitching, W.; Eisenstadt, A.; Brookhart, M. *J. Am. Chem. Soc.* **1979**, *101*, 4896.

(37) Reaction of **13b** with Et_3SiH–CF_3COOH[36c] results in extensive decomposition, while use of $NaBH_4$[38] yields both **14b** and the σ,π-allyl product resulting from attack at C_3.

(38) Eisenstadt, A. *J. Organomet. Chem.* **1976**, *113*, 147.

Table VI

complex	mp, °C	anal., % found C	found H	found N	calc C	calc H	calc N
1b	181–182	67.2	4.36		67.5	4.38	
1c	145–146	68.8	5.24		68.9	5.17	
1d	136–138	68.9	5.31		68.9	5.17	
(6*S*)-**1e**	156–157	68.6	6.62		68.6	6.46	
15[a]	147–149	64.5	5.23		64.8	5.22	
4b	178–181 (dec)	63.9	3.92	6.69	64.1	3.97	6.41
(6*S*)-**4e**	149–151 (dec)	65.1	5.83	5.93	65.3	5.58	5.86
7b	158–159 (dec)	64.8	3.29	9.21	65.1	3.45	9.21
(6*S*)-**7e**[b]	144–145 (dec)	66.2	5.75	7.59	65.9	5.13	7.69
8b	207–209	60.5	4.16	4.29	60.9	4.15	4.31
9b	225–226	61.2	3.87	4.33	60.9	4.15	4.31
(6*S*)-**9e**	135–137	62.3	5.47	4.01	62.4	5.76	3.93
10b	184–185	59.6	4.42	4.25	59.8	4.55	4.11
11b	202–204	59.2	4.20	4.05	59.3	4.34	4.19
(6*S*)-**11e**	157–159	60.9	5.87	3.94	60.8	5.89	3.84
13b	155–157 (dec)	52.0	3.55		51.8	3.51	
(6*S*)-**13e**	142–143	67.3	4.92		67.2	4.77	
14b	137–139	54.3	5.19		54.1	5.23	
(6*S*)-**14e**	133–135	68.1	6.96		68.3	6.80	

[a] Includes 1 mol of CH_3CO_2Et of solvation. [b] Includes 1 mol of acetone of solvation.

perature yields the methyl ethers **12b,e**, which can be converted to the isolated PF_6^- salts **13b,e** by treatment with aqueous HPF_6. ^{31}P spectra of **12e** and **13e** show clearly no loss of planar chirality during these reactions. Reduction of **13b,e** with $NaBH_3CN$ proceeds smoothly to give **14b,e**.[36] The CD spectrum of **14e** (Figure 4) confirms the retention of the 6*S* planar chirality expected for overall addition of H_2 to the uncoordinated double bond of (6*S*)-**1e**.

Experimental Section

All reactions were performed with use of distilled, degassed solvents under a nitrogen atmosphere; (tropone)$Fe(CO)_3$,[36d] (cyclohexadienone)$Fe(CO)_3$,[39] TET,[40] and NMDPP[41] were prepared by literature methods. The NMDPP used contained about 10% of phosphine oxide as an impurity. TCNE and NPTD were sublimed before use; FSO_3H was distilled before use. IR spectra were run on a Perkin-Elmer 257 spectrometer and NMR spectra on either a JEOL FX100 or Bruker AM300 spectrometer, the latter equipped with an ASPECT 3000 data system.

(a) Synthesis of (tropone)$Fe(CO)_2PPh_3$ (1b). (tropone)-$Fe(CO)_3$ (1.4 g, 5.69 mmol) and PPh_3 (2.3 g, 8.78 mmol) were dissolved in acetone (50 mL), and Me_3NO (1.1 g, 9.91 mmol) was added with vigorous stirring. The mixture was refluxed and monitored by infrared spectroscopy and TLC until disappearance of the starting material was essentially complete (ca. 3 h with further periodic addition of more Me_3NO (1.18 g, 10.6 mmol in total)). Diethyl ether (50 mL) was added, and the mixture was filtered through Celite. After removal of solvent, the residue was extracted with 1:1 ethyl acetate–petroleum ether (30–40 °C). After filtration and removal of solvent, the residue was purified by chromatography on alumina with 1:1 ethyl acetate–petroleum ether (30–40 °C) to give, after recrystallization from ethyl acetate–petroleum ether (30–40 °C), (tropone)$Fe(CO)_2PPh_3$ as red crystals (1.67 g, 61%).

Complexes **1c–e** and **15** were prepared in a similar manner. Unreacted NMDPP was removed from **1e** before chromatography by treatment of a diethyl ether solution of the crude product with MeI. Diastereoisomer separation of **1e** was accomplished by dissolution of 1.5 g of (6*S*,*R*)-**1e** in 38 mL of 8:2 ethyl acetate–petroleum ether (30–40 °C) at 65 °C. Crystallization at 5 °C for 48 h yielded 0.18 g of (6*S*)-**1e**.

The rate of diastereoisomer interconversion was measured at 306 K from the ratio of the integrated intensities of the ^{31}P NMR resonances of the two diastereoisomers (ρ) as a function of time. For the equilibrium

$$A \underset{k_{-1}}{\overset{k_1}{\rightleftharpoons}} B$$

(where A represents the 6*S* diastereoisomer isolated by crystallization), a plot of $\ln [(\rho_\alpha - \rho_t)/(\rho_t + 1)] + \ln [(\rho_0 + 1)/(\rho_\alpha - \rho_0)]$ against time[42] yields a vlaue of $k_1 + k_{-1} = 6.8 \times 10^{-4}$ s^{-1}, which for $k_1/k_{-1} = 1.4$ gives $k_1 = 4.0 \times 10^{-4}$ s^{-1} and $k_{-1} = 2.8 \times 10^{-4}$ s^{-1}.

(b) Kinetic Monitoring of Cycloaddition and Isomerization Reactions of 1b with NPTD. Complex **1b** and NPTD were dissolved separately in acetone-d_6 and mixed at 195 K to provide a solution 40 mmol dm^{-3} in **1b** and approximately 30 mmol dm^{-3} in NPTD. The reaction was performed with excess **1b** since even freshly sublimed NPTD undergoes some decomposition on standing for short periods; the exact initial concentration of NPTD (20 mmol dm^{-3}) was calculated from the concentration of **1b** remaining after complete reaction.

After placement in the NMR probe at 237 K, the reaction mixture was monitored by using the relative integrations of the ^{31}P NMR resonances due to **1b**, **2b**, **3b**, and **4b** (Table V). After conversion to concentrations, a plot of time versus $\{1/[A]_0 - [B]_0\} \ln \{[A]_t[B]_0/[A]_0[B]_t\}$ (where A and B represent **1b** and NPTD, respectively) yielded k_1(Scheme I) = $(1.23 \pm 0.18) \times 10^{-2}$ mol^{-1} dm^3 s^{-1}.

Sigmahaptotropic rearrangements were monitored by dissolution of **1b** and excess NPTD separately in acetone-d_6 at 195 K (37 and 40 mmol dm^{-3}, respectively). After the solution was placed in the NMR probe at 264 K, the rearrangement of the initial 1,3-adduct **2b** was monitored by using the relative integration of ^1H NMR resonances; rate constants were evaluated by means of a best-fit computer simulation.

(c) Preparation of NPTD and TCNE Cycloadducts. Complex **1b** (0.25 g, 0.52 mmol) was dissolved in toluene (20 mL) and cooled to 0 °C; NPTD (0.1 g, 0.57 mmol) was added and the mixture stirred for 1 h. After removal of solvent, the product was crystallized from CH_2Cl_2–petroleum ether (30–40 °C) to give **4b** as an off-white powder (0.12 g, 35%). The TCNE adduct **7b** was prepared in a similar way at 25 °C with CH_2Cl_2 as solvent, followed by crystallization from acetone–petroleum ether (30–40 °C). Adducts of (6*S*)-**1e** were prepared in a similar way at 0 °C to minimize racemization.

(d) Preparation and Reactions of Adducts of 1b with TET. (tropone)$Fe(CO)_2PPh_3$ (0.3 g, 0.63 mmol) was dissolved in CH_2Cl_2 (20 mL) at room temperature; TET (0.124 g, 0.626 mmol) was

(39) Birch, A. J.; Chamberlain, K. B. *Organic Syntheses*; Wiley: New York, 1988; Collect. Vol. VI, p 996.
(40) Boger, D. L.; Coleman, R. S.; Panek, J. S.; Huber, F. X.; Sauer, J. *J. Org. Chem.* **1985**, *50*, 5377.
(41) Morrison, J. D.; Masler, W. F. *J. Org. Chem.* **1974**, *39*, 270.
(42) Dixon, D. T.; Kola, J. C.; Howell, J. A. S. *J. Chem. Soc., Dalton Trans.* **1984**, 1307.

added, and after 20 min of stirring, the solvent was evaporated and the residue crystallized from CH_2Cl_2–petroleum ether (30–40 °C) to give **8b** (0.399 g, 86%) as an orange solid. Addition of 1 drop of CF_3COOH to a dichloromethane solution of **8b**, followed by chromatography on silica gel with ethyl acetate and crystallization from CH_2Cl_2–MeOH, gave **9b** (96%) as a yellow solid. The isomerization may be effected thermally by reflux of a solution of **8b** in 1:1 toluene–$CHCl_3$ overnight. Crystallization of **8b** from CH_2Cl_2–MeOH yields the methanol adduct **10b** (66%), while the hydrate **11b** may be prepared by reaction of (tropone)Fe(CO)$_2$PPh$_3$ (0.2 g, 0.42 mmol) with TET (0.083 g, 0.42 mmol) in 25 mL of 1% water–acetone (acetone previously dried by distillation from $MgSO_4$) at room temperature for 3 h. Removal of solvent followed by chromatography on Florisil with 1:1 acetone–petroleum ether (30–40 °C) and by crystallization from ethyl acetate–petroleum ether (30–40 °C) gave **11b** (76%) as a yellow solid. Reaction of (6*S*)-**1e** with TET at 0 °C gave **8e**, characterized spectroscopically. Conversion to **9e** and preparation of **11e** were accomplished as described for **1b**.

(e) Preparation of (cycloheptadienone)Fe(CO)$_2$PPh$_3$ (14b). (tropone)Fe(CO)$_2$PPh$_3$ (0.35 g, 0.729 mmol) was dissolved in CH_2Cl_2 (60 mL) and cooled to −78 °C; to this was added HSO_3F (1 mL) in CH_2Cl_2 (2 mL) precooled to −78 °C. After several minutes, the dark red-brown color faded to pale yellow and the solution was poured into a suspension of Na_2CO_3 (5 g) in MeOH (10 mL) at −78 °C. After it was warmed to room temperature, the mixture was diluted with water (10 mL) and extracted with CH_2Cl_2 (2 × 35 mL). After being washed with water and saturated NaCl, the extracts were dried ($MgSO_4$) and evaporated to give **12b** (75%), characterized spectroscopically (Table II). Complex **12b** (0.22 g, 0.43 mmol) was dissolved in CH_2Cl_2 (1 mL) and cooled to 0 °C; with stirring, 75% HPF_6 (0.09 ml) was added, followed after 20 min by diethyl ether (10 mL) to precipitate **13b** (78%), which was filtered and recrystallized from CH_2Cl_2/diethyl ether. Complex **13e** was prepared in the same way.

Complex **13b** (0.85 g, 1.36 mmol) was dissolved in THF (220 mL) and cooled to −78 °C; to this was added $NaBH_3CN$ (0.17 g, 2.71 mmol) in THF (340 mL) precooled to −78 °C. After it was stirred for 15 min, the mixture was warmed to room temperature and stirred for 2 h. After removal of solvent, the residue was dissolved in CH_2Cl_2 (200 mL) and washed with water and saturated NaCl. After drying ($MgSO_4$) and removal of solvent, the residue was chromatographed on alumina with 1:3 ethyl acetate–petroleum ether (30–40 °C) to give **14b** (55%) as an orange solid, recrystallized from ethyl acetate–petroleum ether (40–60 °C). Complex **14e** was obtained similarly.

(f) Crystal Structure Determination of 1b ($C_{27}H_{21}FeO_3P$). Diffraction data were measured at ca. 18 °C on an CAD4 diffractometer equipped with a graphite monochromator, using Mo Kα (λ = 0.71069 Å) radiation. The unit-cell constants were determined by least squares from 25 accurately positioned reflections. The intensities of reflections within $0 < 2\theta < 50°$ ($(\sin\theta)/\lambda < 0.60$ Å^{-1}) were collected by the ω–2θ scan technique with a scan range of $(1.0 + 0.3 \tan\theta)°$. All data were recorded at a constant 3° min^{-1} scan rate. Possible deterioration of the analyzed crystals was tested by detecting frequently the intensities of standard reflections and was found to be negligible during the measurements. The data sets were not corrected for absorption or secondary extinction effects.

The compound crystallizes in the triclinic space group $P\bar{1}$, with two molecular entities in the unit cell (Z = 2). The crystal data are as follows: M_r = 480.3; a = 8.789 (1), b = 11.212 (6), c = 12.889 (3) Å; α = 64.43 (2), β = 75.92 (2), γ = 80.98 (2)°; V = 1109,4 Å^3; d_c = 1.438 g cm^{-3}; μ(Mo Kα) = 7.75 cm^{-1}; F(000) = 496.

The structure was solved by a combination of direct methods and Fourier techniques (MULTAN80). The refinement was carried out by large-block least squares (SHELX76), including the positional and anisotropic thermal parameters of all the non-hydrogen atoms. The phenyl substituents were treated in the refinement calculations as geometrically constrained rigid groups, to avoid unreliable distortions in their geometry due to the effects of thermal motion. All hydrogens were included in the structure factor computations in calculated positions, the phenyl groups being treated as rigid groups. The final refinements were based only on those observations that satisfied the condition $F^2 > 3\sigma(F^2)$, with use of experimental weights ($w = \sigma^{-2}(F_o)$) and minimization of $w(\Delta F)^2$. The final difference-fourier maps showed no indication of incorrectly placed or missing atoms, the highest peak and deepest trough not exceeding 0.6 e Å^{-3}. At convergence the discrepancy factors are R = 0.057 for 2564 reflections above the intensity threshold (out of 3567 unique data above zero) and a goodness of fit of 1.42 e. The final atomic coordinates of the non-hydrogen atoms are listed in Table IV. Drawings and bond length and bond angle data for **1a** and for (1,2,4,6-tetraphenyltropone)Fe(CO)$_3$ were generated from the literature atomic coordinates.[19]

Acknowledgment. We thank Dr. A. F. Drake (University College, London) for the CD spectra, Dr. T. A. Albright for discussion, and Dafna Hezroni for crystallographic computations.

Supplementary Material Available: Listings of atomic coordinates of the hydrogen atoms, bond lengths and angles, and anisotropic thermal parameters of the non-hydrogen atoms (4 pages); a table of observed and calculated structure factors (9 pages). Ordering information is given on any current masthead page.